A mixing model for turbulent flows based on parameterized scalar profiles

D. W. Meyer and P. Jenny

Citation: Physics of Fluids **18**, 035105 (2006); doi: 10.1063/1.2182005
View online: http://dx.doi.org/10.1063/1.2182005
View Table of Contents: http://scitation.aip.org/content/aip/journal/pof2/18/3?ver=pdfcov
Published by the AIP Publishing

A mixing model for turbulent flows based on parameterized scalar profiles

D. W. Meyer[a] and P. Jenny[b]
Institute of Fluid Dynamics, ETH Zürich, Sonneggstrasse 3, 8092 Zürich, Switzerland

(Received 14 July 2005; accepted 24 January 2006; published online 16 March 2006)

In this paper the closure of molecular mixing in turbulent reactive flows is addressed in the context of probability density function methods. It is safe to say that the lack of a general and accurate mixing model is a major source for uncertainties in turbulent combustion simulation. Here, we propose a model based on constructing statistical distributions of one-dimensional scalar profiles, i.e., fluid particles are associated to parameterized scalar profiles (PSP). Opposed to previous approaches, the PSP model results in a simple formulation and is able to produce very accurate results at low computational cost. For validation, a two-scalar mixing problem in homogeneous isotropic turbulence was used. The accuracy of the PSP model was demonstrated by comparison with direct numerical simulation data and confirms that the intrinsic physical assumptions are justified. © *2006 American Institute of Physics*. [DOI: 10.1063/1.2182005]

I. INTRODUCTION

Probability density function (PDF) methods are in particular attractive due to the fact that turbulence-reaction interaction appears in closed form.[1] If the joint velocity-composition PDF (JPDF) transport equation is solved, an additional advantage over second moment closure methods is that the turbulent transport terms do not have to be modeled either, e.g., no gradient diffusion model has to be employed. With the recent development of efficient solution algorithms[2] it was demonstrated[3] that it is feasible to apply the JPDF approach for turbulent reactive flow applications in industry on a more regular basis. From a modeling viewpoint, one of the biggest challenges is a general and accurate model for the description of molecular mixing (or micromixing) of scalars like temperature and species mass fractions. These processes occur at the smallest scales and the difficulties involved in their description are enormous.[4] Fox,[5] Pope,[1] and Subramaniam and Pope[6] suggest the following criteria that should be satisfied by an ideal mixing model:

(i) the mean of the scalars must remain unchanged,
(ii) the variance of the scalars must decrease,
(iii) in homogeneous turbulence the joint PDF of inert scalars should relax to a joint Gaussian,
(iv) realizability has to be honored, i.e., scalars have to remain within their convex hull,
(v) insensitivity with respect to linear transformations in scalar space and independence of passive scalars,
(vi) localness in scalar space,
(vii) correct dependence on scalar length scales, and
(viii) correct dependence on Reynolds, Schmidt, and Damköhler numbers.

Norris and Pope[7] have demonstrated that criterion (vi) is of particular importance in reactive flows, e.g., combustion. Subramaniam and Pope[6] argue that particles should mix with other particles in their immediate neighborhood in scalar space. The rationale for this requirement is based on the fact that, for smooth scalar fields, neighboring particles in physical space are also adjacent in scalar space. Fox[5] describes a weaker form of localness, which only requires that scalars vary smoothly with time. An additional criterion for a successful mixing model is that it should produce accurate results at low computational cost. Moreover, rather than using an *ad hoc* approach, a more physical basis is preferable since that would result in more straightforward extensions. In terms of accuracy, a mixing model should be able to reliably predict the evolution of joint scalar one-point, one-time PDFs (Eulerian correspondence). Direct numerical simulation (DNS) data of appropriate test cases, which consider mixing in homogeneous isotropic turbulence, was made available by Juneja *et al.*[8,9] Also important for the development of mixing models are Lagrangian scalar statistics, e.g., from DNS.[10]

The earliest attempts to model molecular mixing were those by Curl,[11] who proposed the coalescence-dispersion (CD) model, and by Villermaux and Devillon,[12] who developed the interaction by exchange with the mean (IEM) model. The latter is also referred to as linear mean-square estimation model by Dopazo and O'Brien.[13] These models fulfill criteria (i), (ii), (iv), and (v). However, both models do not relax to a Gaussian PDF [criterion (iii)] and are not local in scalar space [criterion (vi)]. The most important deficiency of the IEM model is that it preserves the shape of the PDF, which is a severe violation of the physics. While this can lead to very bad results in homogeneous turbulence, it has to be mentioned that this deficiency is less dramatic for inhomogeneous turbulent mixing scenarios. This is due to macromixing, which also affects the shape of the local scalar PDFs. Therefore, and due to its simplicity and efficiency, the IEM model still is the most widely used mixing model. More recently, Pope[14] introduced the mapping closure (MC) model for a single scalar. Major improvements of this mixing model are that it fulfills the localness criterion (vi) and that it is

[a]Electronic mail: meyer@ifd.mavt.ethz.ch
[b]Electronic mail: jenny@ifd.mavt.ethz.ch

more accurate than previous ones. Later, Subramaniam and Pope[6] devised a mixing model based on constructing Euclidean minimum spanning trees (EMST) in scalar space to deal with the localness condition in the case of multiple scalars. In a sense, one can regard the EMST model as a multiscalar extension of the MC implementation. This extension is quite involved and not straightforward, however. The most important advantage of the EMST model is that mixing is treated locally in the multidimensional scalar space, which is of particular importance for turbulent combustion. The EMST mixing model was successfully applied to different combustion problems.[15–18] More recently, Klimenko and Pope[19] presented the multiple mapping conditioning (MMC) model, which is a multidimensional extension of the MC. Another modeling approach, based on Fokker–Planck (FP) equations, was introduced by Fox.[20–22] Comparison with DNS data revealed that the FP models work satisfactory in many cases. In general, however, the boundedness requirement (iv) is not fulfilled. Analogously to the FP models, Heinz[23] proposed to add a diffusion term to the IEM model. Accordingly he refers to this modification as stochastic IEM (SIEM) mixing model.[24] It has to be mentioned that there exists little experience with the FP and MMC models in combination with practical studies. In summary, it can be said that the closure of the molecular mixing term remains one of the biggest challenges in PDF modeling of turbulent reactive flows. Therefore, and due to its importance, the development of general and accurate mixing models will remain an active research area for some time to come.[25]

In this paper we present a distinctly different approach for the closure of molecular mixing in turbulent flow. Unlike previous ones, our new model is based on a statistical construction of a physical picture at the smallest scales. The scalar fields are characterized by a distribution of one-dimensional scalar profiles and their temporal evolution. Therefore, a number of assumptions are made. First, the profiles are parameterized. They are approximated by a self-similar shape specified by a length scale, a minimum and a maximum value. For an appropriate evolution of these parameters, stochastic processes were formulated. Comparison with DNS data of passive scalar mixing shows that this parameterized scalar profile (PSP) mixing model is very accurate, general, and efficient. It was also demonstrated, using a challenging test case, that the PSP mixing model has no difficulty in handling multiscalar mixing.

In Sec. II of this paper, the basic PDF framework and in Sec. III, the details of the PSP mixing model are explained. Numerical experiments and results are presented in Sec. IV. In particular, the PSP model is validated with DNS data of multiscalar mixing in homogeneous isotropic turbulence.[8] Finally, concluding remarks are found in Sec. V.

II. PDF MODELING FRAMEWORK

In this section we briefly describe the basic principles of PDF methods and the role of the mixing model. Therefore, we consider a turbulent flow field with the instantaneous velocity $\mathbf{U}(\mathbf{x},t)$ and the composition $\phi(\mathbf{x},t)$. First, everything is explained for constant density flow and one scalar with constant diffusion coefficient, Γ. Later, in Sec. III B 3, a generalization to multiple scalars is presented. The evolution of the scalar ϕ can be expressed as

$$\frac{\partial \phi}{\partial t} + \mathbf{U} \cdot \nabla \phi = \Gamma \nabla^2 \phi + S(\phi), \tag{1}$$

where $S(\phi)$ is the reaction source term. In composition PDF methods, one-point, one-time PDFs of ϕ are considered at each location, $\mathbf{x}$, and time, t. The exact transport equation of the composition PDF, $f_\phi(\psi;\mathbf{x},t)$, can be derived from Eq. (1) (Refs. 1 and 5); it reads

$$\frac{\partial f_\phi}{\partial t} + \nabla \cdot (\langle \mathbf{U}|\psi\rangle f_\phi) = -\frac{\partial}{\partial \psi}(\langle \Gamma \nabla^2 \phi|\psi\rangle f_\phi) - \frac{\partial}{\partial \psi}[S(\psi) f_\phi], \tag{2}$$

where ψ is the sample space coordinate of ϕ and $\langle\cdot|\psi\rangle$ denotes a conditional expectation. Note that in addition to $\mathbf{x}$ and t, ψ also is an independent variable. In fact, Eq. (2) is a high dimensional transport equation, especially if multiple scalars are considered ($n+4$ dimensions, where n is the number of scalars). Therefore, such PDF transport equations are usually solved with particle methods.[1,5] More precisely, notional particles with certain properties, e.g., composition, $\phi^{(i)}$, and position, $\mathbf{x}^{(i)}$, are evolved in physical and sample space. The superscript (i) indicates that the quantity is a property of the particle with index i. The stochastic differential equations (SDE), which describe the evolution of the particle properties, are constructed such that the notional particles mimic the behavior of the fluid particles.

The most remarkable property of Eq. (2) is the fact that chemical reaction appears in closed form [the term with the source $S(\psi)$]. However, models are required for the conditional expectations. Here, it is worthwhile to mention that full PDF closure can be obtained by joint velocity-frequency-composition PDF methods. In that case, an additional advantage is that also turbulent transport appears in closed form. Moreover, the turbulence frequency provides the necessary time scale to model the unclosed terms. In this paper only the closure of conditional diffusion is discussed.

III. PARAMETERIZED SCALAR PROFILE MIXING MODEL

The basic idea behind the PSP mixing model is the parameterization of one-dimensional scalar profiles. Since, in some respect, it can be regarded as a generalization of the IEM model, we first give a physical interpretation of the IEM mixing model.

A. Physical interpretation of the IEM model

Conditional diffusion of a single scalar is described by the IEM model[12,13] as

$$\langle \Gamma \nabla^2 \phi|\psi\rangle = -\tfrac{1}{2} C_\phi \langle \omega \rangle (\psi - \langle \phi \rangle), \tag{3}$$

where $\langle\omega\rangle$ is the mean turbulence frequency and C_ϕ is a model constant, assuming a constant mechanical-to-scalar time scale ratio. Correspondingly, employing the IEM model, the evolution of the particle i in scalar space due to mixing is

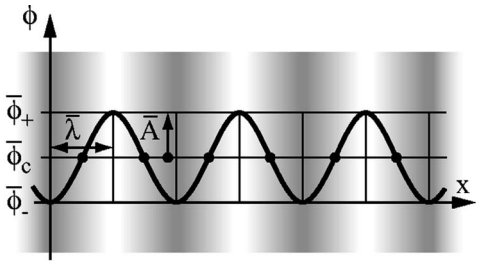

FIG. 1. Lamellar structure of scalar profiles assumed by the IEM model (dark=low scalar value).

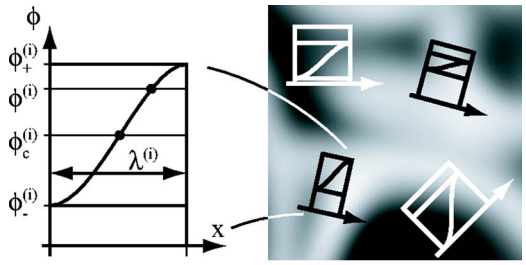

FIG. 2. Parameterized scalar profile of particle i and sketch of different profiles in a planar slice through a turbulent flow (dark=low scalar value).

$$\frac{d\phi^{(i)}}{dt} = -\frac{1}{\bar{\tau}_\phi}(\phi^{(i)} - \langle\phi\rangle), \tag{4}$$

where $\bar{\tau}_\phi = 2/(C_\phi\langle\omega\rangle)$ is a mixing time scale. Comparing the right-hand side of Eq. (4) with that of

$$\frac{d\phi^{(i)}}{dt} = \Gamma\frac{\partial^2\phi^{(i)}}{\partial x_j\,\partial x_j}, \tag{5}$$

according to Eq. (1), and assuming one-dimensional diffusion leads to the ordinary differential equation

$$\Gamma\frac{\partial^2\phi^{(i)}}{\partial x^2} = -\frac{1}{\bar{\tau}_\phi}(\phi^{(i)} - \langle\phi\rangle). \tag{6}$$

A possible solution to this equation is given by[26]

$$\phi^{(i)}(x,t) = \bar{A}e^{-t/\bar{\tau}_\phi}\sin(\pi x/\bar{\lambda}) + \bar{\phi}_c, \tag{7}$$

where $\bar{A}$ is an amplitude, $\bar{\lambda} = \pi\sqrt{\Gamma\bar{\tau}_\phi}$ is a length scale and $\bar{\phi}_c = \langle\phi\rangle$ is a profile center value. Note that solution (7) satisfies both Eqs. (4) and (5). The conclusion from this analysis is that the IEM mixing model predicts the correct evolution of a scalar ϕ, if all fluid particles are located on one-dimensional sinusoidal scalar profiles with the same length scale and the same profile center value, in other words, if the spatial scalar distribution has a lamellar structure as illustrated in Fig. 1. While one can argue that the assumption of one-dimensional sinusoidal scalar profiles is justified (at least for inert scalars), it certainly is not true that all profiles can be characterized by the same length scale and center value.

B. Generalization of the IEM model: The PSP mixing model

The basic ideas of the PSP mixing model deal with a more general parameterization of the one-dimensional scalar profiles, i.e., instead of using the same parameters $\bar{\lambda}$ and $\bar{\phi}_c$ for all profiles, models for individual length scales, λ, and center values, ϕ_c, are proposed. A sketch of such a parameterized scalar profile is shown in Fig. 2. A similar approach was suggested by Fox.[20] From his considerations of using different amplitudes and different length scales (in his paper $C_{\max}$ and Y, respectively) he derived a FP model. Other than in the approach by Fox, in the PSP model additional stochastic processes for the parameters λ, ϕ_-, and ϕ_+ (which are the minimum and maximum values on the profile, respectively) are formulated. The relation between the profile center value, ϕ_c, and the profile boundary values, ϕ_- and ϕ_+, is simply given by

$$\phi_c^{(i)} = \frac{\phi_+^{(i)} + \phi_-^{(i)}}{2}. \tag{8}$$

The introduction of additional scalar processes for the profile parameters results in a higher level of closure. In fact, each particle carries additional properties, i.e., the parameters λ, ϕ_-, and ϕ_+. It has to be mentioned, however, that λ can be modeled as a function of the turbulence frequency, ω. In joint velocity-frequency-composition PDF methods, for example, the turbulence frequency is already modeled and therefore ϕ_+ and ϕ_- are the only additional particle properties. Finally, if this form of parameterization is accepted, molecular mixing itself appears in closed form and the evolution of the scalar ϕ can be described by

$$\frac{d\phi^{(i)}}{dt} = -\frac{1}{\tau_\phi^{(i)}}(\phi^{(i)} - \phi_c^{(i)}) + S(\phi^{(i)})$$
$$\text{with} \quad \tau_\phi^{(i)} = 2/(C'_\phi\omega^{(i)}). \tag{9}$$

Note the similarity with the IEM model and that a new model constant C'_ϕ (which is different than C_ϕ) was introduced. Next, we discuss the processes that describe the evolution of the profile parameters.

The turbulence frequency, which is related to the profile length scale as

$$\lambda^{(i)} = \pi\sqrt{\frac{2\Gamma}{C'_\phi\omega^{(i)}}}, \tag{10}$$

can be modeled by the SDE

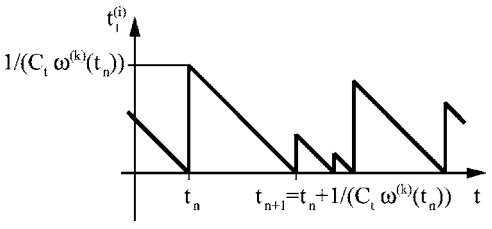

FIG. 3. Evolution of time stamp $t_+^{(i)}$.

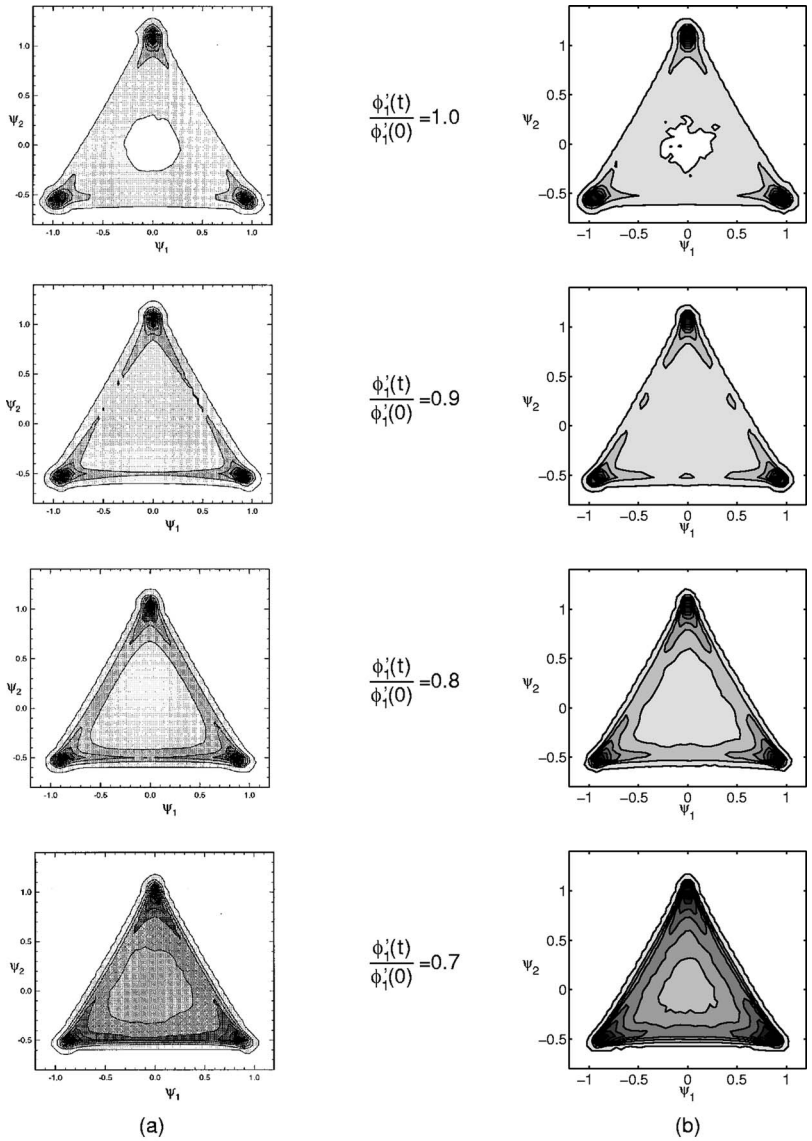

FIG. 4. Joint PDF, $f_{\phi_1,\phi_2}(\psi_1,\psi_2;t)$, phase 1; (a) DNS R92A by Juneja and Pope (Ref. 8), (b) PSP mixing model; the ten contour levels range from 0.01 to 1 (black) and represent the PDF normalized by its maximum value.

$$d\omega^{(i)} = -(\omega^{(i)} - \langle\omega\rangle)\frac{dt}{T_\omega} + \sqrt{\frac{2\sigma^2\langle\omega\rangle\omega^{(i)}}{T_\omega}}dW, \tag{11}$$

where the time scale is taken to be $T_\omega = 1/(C_3\langle\omega\rangle)$, σ^2 is the variance of $\omega^{(i)}/\langle\omega\rangle$ and $W(t)$ is a Wiener process. This is the gamma-distribution model suggested by Jayesh and Pope[27] to get a time scale for joint velocity-frequency-composition PDF methods. Equation (11) is the form for statistically stationary isotropic turbulence. Note that other processes for ω have been devised,[28] but that an appropriate autocorrelation time scale and a reasonable distribution for ω are always crucial.

1. Profile boundaries

Our model for the profile boundaries, ϕ_- and ϕ_+, is based on the approximation that the PDF of ϕ_- and ϕ_+ combined is the same as for ϕ. With this assumption it becomes natural to represent $\phi_-^{(i)}$ and $\phi_+^{(i)}$ of particle i by the scalars $\phi^{(j)}$ and $\phi^{(k)}$ of two other particles, j and k, respectively, both from the same computational cell as particle i and both evolving like particle i in scalar space. Thereby, one has to ensure that condition

$$(\phi_-^{(i)} - \phi^{(i)})(\phi_+^{(i)} - \phi^{(i)}) \leqslant 0 \tag{12}$$

is satisfied. Note that Eq. (12) is equivalent to either $\phi_-^{(i)} \leqslant \phi^{(i)} \leqslant \phi_+^{(i)}$ (displayed in Fig. 2) or $\phi_-^{(i)} \geqslant \phi^{(i)} \geqslant \phi_+^{(i)}$. As a consequence, the scalar profile associated with particle i is considered degenerated as soon as requirement (12) is violated. In that case, new representatives for $\phi_-^{(i)}$ and $\phi_+^{(i)}$ are chosen as following: particle pairs are randomly selected and the first pair satisfying condition (12) is chosen. In addition, it is also necessary to account for decorrelation with time. This is achieved by a similar reinitialization procedure, but now triggered spontaneously by intermittent aging processes based on the turbulence frequency. Each particle i carries two time stamps, $t_-^{(i)}$ and $t_+^{(i)}$, which decrease with time. For example, if $t_+^{(i)}$ has become zero or negative a new representative particle k is randomly selected for $\phi_+^{(i)}$ from the subensemble of particles satisfying condition (12), i.e., $\phi_+^{(i)}$

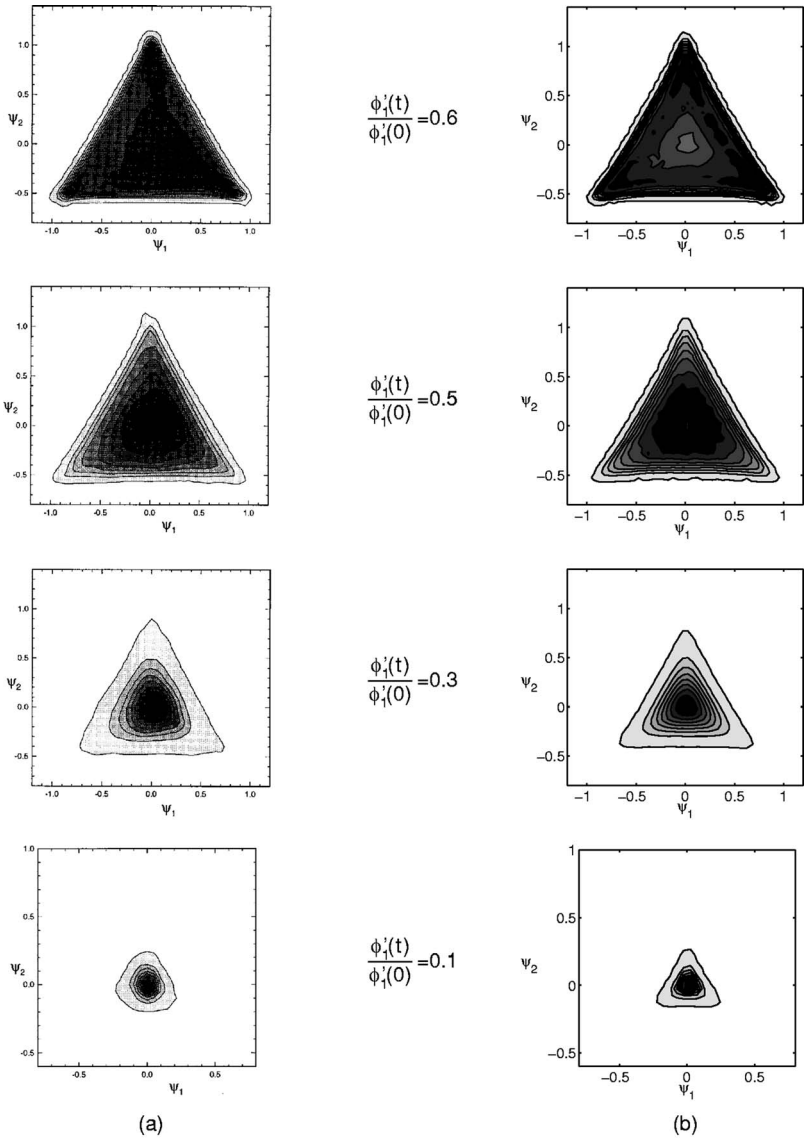

FIG. 5. Joint PDF, $f_{\phi_1,\phi_2}(\psi_1,\psi_2;t)$, phase 2; same as Fig. 4.

$=\phi^{(k)}$. Additionally, $t_+^{(i)}$ is set to $1/(C_t\omega^{(k)})$, where C_t is a model constant. A sketch showing the evolution of $t_+^{(i)}$ is given in Fig. 3. Note that $\phi_-^{(i)}$ is treated analogously with $t_-^{(i)}$.

An efficient implementation of the discussed renewal processes is outlined in Appendix A.

2. Conservation of mean

It is important for any mixing model that conservation of the scalars is not violated, i.e., the mean of the scalar has to be preserved [criterion (i)]. Fox[29] suggests "a time-dependent shift and rescale operation" to correct conservation errors introduced by the FP model. The approach presented next is based on similar ideas and can be applied in combination with any mixing model that does not fulfill criterion (i) automatically. Considering n_p particles, the change of the mean ϕ due to the mixing model is

$$\langle d\phi\rangle = \frac{1}{n_p}\sum_{i=1}^{n_p} d\phi^{(i)}. \tag{13}$$

Note that, in order to be conservative, $\langle d\phi\rangle$ should be zero. To correct any deviation from that, the individual changes, $d\phi^{(i)}$, are multiplied by a factor $\alpha^{(i)}$, which leads to the new requirement:

$$\frac{1}{n_p}\sum_{i=1}^{n_p} \alpha^{(i)} d\phi^{(i)} = 0, \tag{14}$$

where $\alpha^{(i)}d\phi^{(i)}$ are the modified changes. The choice of the scaling factors $\alpha^{(i)}$ is subtle since it is not only important to conserve the mean of a scalar, but also to guarantee its boundedness [criterion (iv)]. To satisfy both requirements we compute $\alpha^{(i)}$ as

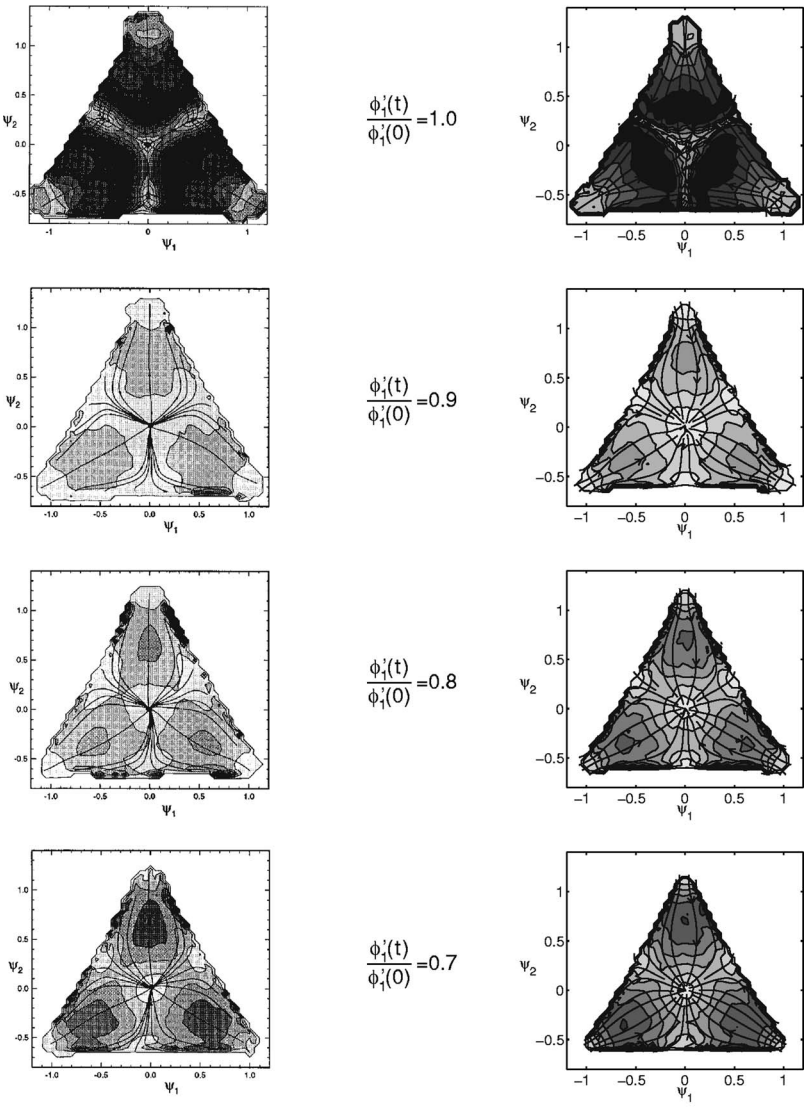

FIG. 6. Conditional scalar diffusion rate, $\boldsymbol{\gamma}(\psi_1,\psi_2;t)$, phase 1; (a) DNS R92A by Juneja and Pope (Ref. 8), (b) PSP mixing model; the ten contour levels range from 0.01 to 1 (black) and represent $|\boldsymbol{\gamma}|$ normalized by its maximum value; the lines are parallel to $\boldsymbol{\gamma}$.

$$\alpha^{(i)}=\begin{cases}-\langle d\phi\rangle_+/\langle d\phi\rangle_- & \text{if} \quad d\phi^{(i)}<0 \quad \text{and} \quad \langle d\phi\rangle<0,\\ -\langle d\phi\rangle_-/\langle d\phi\rangle_+ & \text{if} \quad d\phi^{(i)}>0 \quad \text{and} \quad \langle d\phi\rangle>0,\\ 1 & \text{otherwise},\end{cases} \tag{15}$$

where

$$\langle d\phi\rangle_\pm=\frac{1}{n_p}\sum_{i=1}^{n_p}H(\pm d\phi^{(i)})d\phi^{(i)} \tag{16}$$

using the Heaviside function $H(\cdot)$. Next, we prove that with this choice for $\alpha^{(i)}$ both requirements, conservation and boundedness, are fulfilled. Let us consider the case if $\langle d\phi\rangle<0$. Then, using $\langle \alpha d\phi\rangle=\langle \alpha d\phi\rangle_+ +\langle \alpha d\phi\rangle_-$, the average of the modified changes is

$$\begin{aligned}\frac{1}{n_p}\sum_{i=1}^{n_p}\alpha^{(i)}d\phi^{(i)}&=\frac{1}{n_p}\left(\sum_{i=1}^{n_p}H(d\phi^{(i)})d\phi^{(i)}+\sum_{i=1}^{n_p}H(-d\phi^{(i)})\alpha^{(i)}d\phi^{(i)}\right)\\&=\langle d\phi\rangle_+-\frac{\langle d\phi\rangle_+}{\langle d\phi\rangle_-}\langle d\phi\rangle_-=0,\end{aligned} \tag{17}$$

which proves that the mean is conserved. Moreover, the factor $\alpha^{(i)}$ is always in the range between zero and one, which guarantees boundedness.

3. Multiple scalars

In this section it is shown that the extension of the PSP mixing model from one to multiple scalars is straightforward. Instead of one scalar ϕ we now consider the composition vector $\boldsymbol{\phi}=(\phi_1,\phi_2,\ldots,\phi_n)^T$. Correspondingly, the pro-

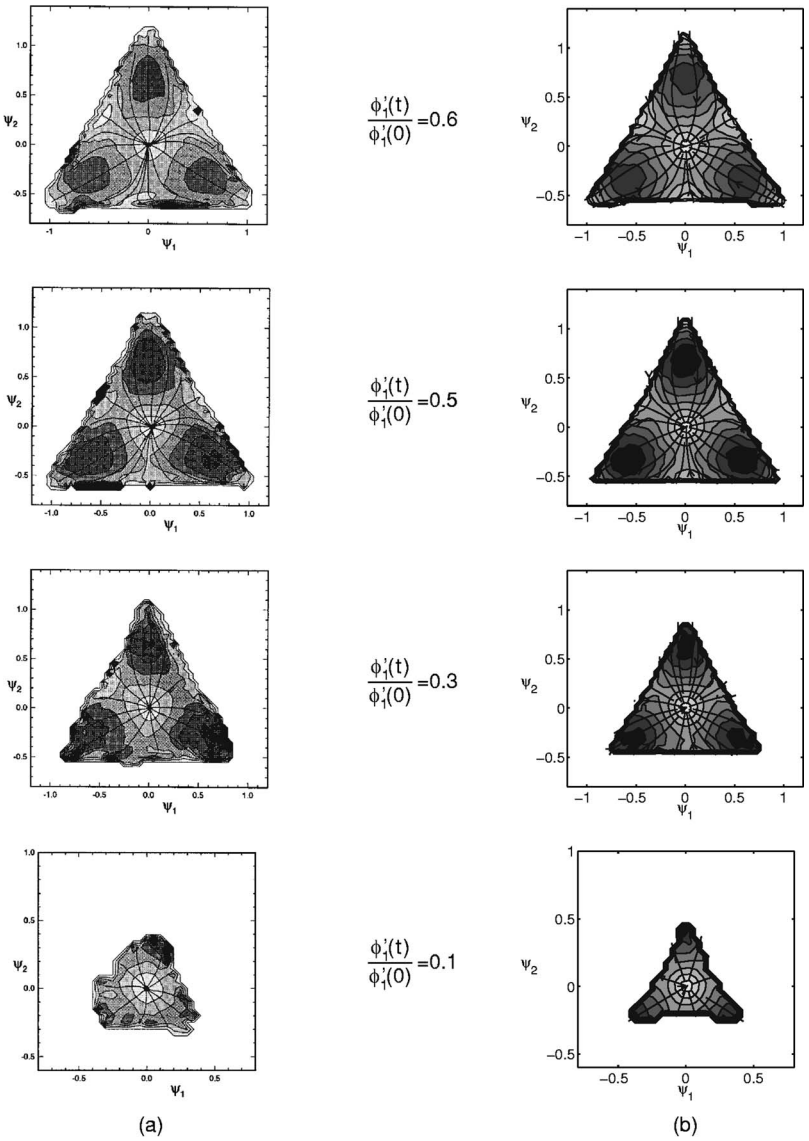

FIG. 7. Conditional scalar diffusion rate, $\gamma(\psi_1,\psi_2;t)$, phase 2; same as Fig. 6.

file boundaries are defined by the vectors $\boldsymbol{\phi}_-$ and $\boldsymbol{\phi}_+$. Analogously to Eq. (9), the evolution of the particle composition vector $\boldsymbol{\phi}$ is given by

$$\frac{d\boldsymbol{\phi}^{(i)}}{dt} = -\frac{1}{\tau_\phi^{(i)}}(\boldsymbol{\phi}^{(i)} - \boldsymbol{\phi}_c^{(i)}) + \mathbf{S}(\boldsymbol{\phi}^{(i)})$$
$$\text{with} \quad \boldsymbol{\phi}_c^{(i)} = \frac{\boldsymbol{\phi}_+^{(i)} + \boldsymbol{\phi}_-^{(i)}}{2}. \tag{18}$$

For the reinitialization procedure of the profile boundaries it is necessary to generalize condition (12). The new condition reads

$$(\boldsymbol{\phi}_-^{(i)} - \boldsymbol{\phi}^{(i)}) \cdot (\boldsymbol{\phi}_+^{(i)} - \boldsymbol{\phi}^{(i)}) \leqslant 0 \tag{19}$$

and becomes identical to condition (12) for $n=1$. Condition (19) is true if the angle between the vectors $\boldsymbol{\phi}_-^{(i)} - \boldsymbol{\phi}^{(i)}$ and $\boldsymbol{\phi}_+^{(i)} - \boldsymbol{\phi}^{(i)}$ is greater or equal $\pi/2$. It is invariant to rotations in scalar space, however, it does not fulfill the linearity criterion (v). Moreover, the picture of self-similar profiles is no longer as simple as depicted in Fig. 2. Another small modification is required in the correction procedure described in Sec. III B 2. To avoid an orientation (in scalar space) dependent bias error, the vector $d\boldsymbol{\phi}$ is transformed into a randomly oriented, orthogonal coordinate system before the correction is applied. The random, orthogonal transformation can be achieved easily by first generating n linearly independent, n-dimensional random vectors. Then, by using the method of Schmidt,[30] one obtains new base vectors, $\mathbf{e}_1, \mathbf{e}_2, \cdots, \mathbf{e}_n$. The transformation is then given by

$$\widetilde{d\boldsymbol{\phi}}^{(i)} = [\mathbf{e}_1 \mathbf{e}_2 \cdots \mathbf{e}_n]^T d\boldsymbol{\phi}^{(i)} \tag{20}$$

and the back transformation of the corrected changes, $\widetilde{d\boldsymbol{\phi}}_{\text{corr}}^{(i)}$, is

$$d\boldsymbol{\phi}_{\text{corr}}^{(i)} = [\mathbf{e}_1 \mathbf{e}_2 \cdots \mathbf{e}_n] \widetilde{d\boldsymbol{\phi}}_{\text{corr}}^{(i)}. \tag{21}$$

Like this, in addition to satisfying conservation, the bias error due to orientation is avoided. Since boundedness is only guaranteed componentwise, the correction procedure not necessarily ensures that all particles remain inside the convex hull of the distribution in the multiscalar sample space. How-

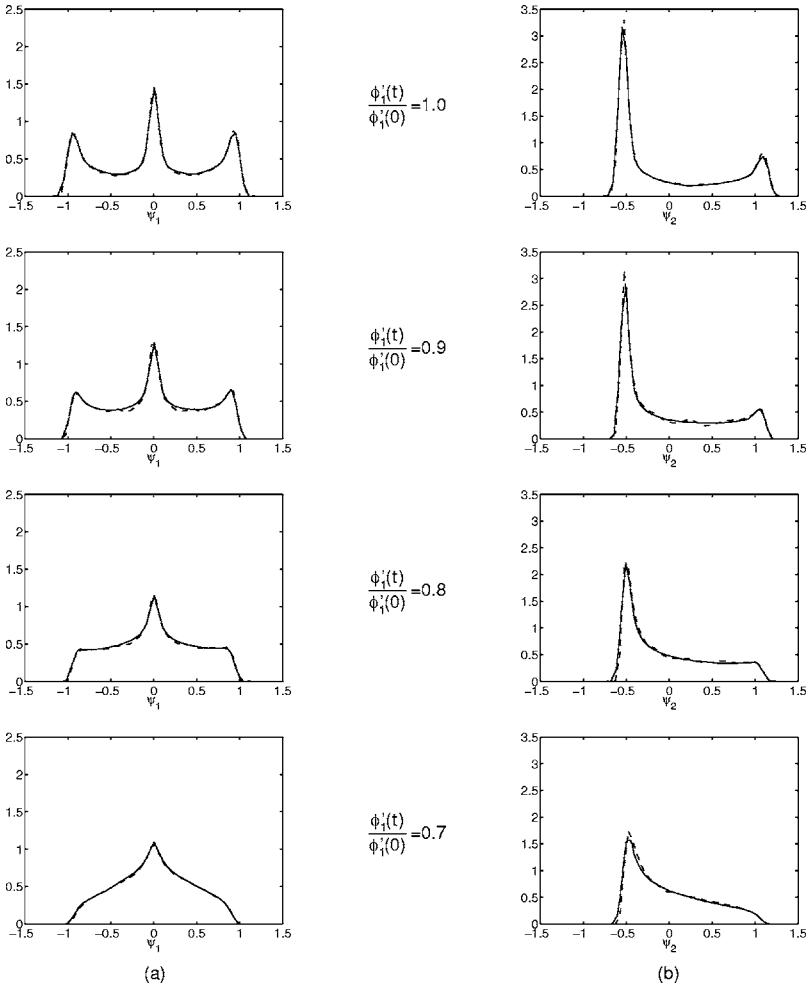

FIG. 8. Marginal PDFs, phase 1; (a) $f_{\phi_1}(\psi_1;t)$, (b) $f_{\phi_2}(\psi_2;t)$; DNS R92A by Juneja and Pope (Ref. 8) (solid lines), PSP mixing model (dashed lines).

ever, since the correction factors, $0 \leqslant \alpha^{(i)} \leqslant 1$, approach 1 for increasing particle numbers, in general boundedness is violated only weakly. Below it is demonstrated that the extension of the PSP mixing model to multiscalar mixing gives excellent results, despite the additional assumptions about the one-dimensional scalar profiles.

IV. VALIDATION

In order to examine how PDFs, using the PSP mixing model, evolve, a numerical simulation of two passive scalars, ϕ_1 and ϕ_2, in homogeneous isotropic turbulence was performed. The results of the zero-dimensional simulation are compared with the DNS data R48A and R92A of Juneja and Pope[8] with Taylor-scale Reynolds numbers $\mathrm{Re}_\lambda = 48.6$ and $\mathrm{Re}_\lambda = 92.4$, respectively. In simulation R48A the mechanical-to-scalar time scale ratio was approximately constant and no differential diffusion was considered. At this point, these are assumptions made by the PSP model. The accuracy with respect to the shape of the joint scalar PDF, $f_{\phi_1,\phi_2}(\psi_1,\psi_2;t)$, was investigated and compared with R92A. Juneja and Pope mention that the joint PDFs of R48A and R92A are very similar and conclude that mixing is not significantly influenced by the Reynolds number in the range considered. Temporal evolutions of global quantities such as scalar root mean square (rms) values, ϕ_1' and ϕ_2', and normalized higher moments were validated with the data from R48A. Another issue is the efficiency of the PSP mixing model that is in inhomogeneous flows tightly related to the number of particles required per grid cell. The main criterion therefore is the deterministic bias error,[2] which was investigated for the PSP model in an extensive study. Furthermore, it was demonstrated that the predictions of the PSP mixing model also depend on the initial conditional scalar diffusion rate.

A. Simulation setup

For all simulations in this paper the turbulence frequency model (11) with $C_3 = 1$ and $\sigma^2 = \langle(\omega - \langle\omega\rangle)^2\rangle / \langle\omega\rangle^2 = 1/4$ was employed. For the initial turbulence frequency, $\omega^{(i)}$, a suitable random number generator was used. Optimal agreement with the DNS was obtained with $C_\phi' = 25$ and $C_t = 2$. In order to ensure that departures from DNS data is less due to statistical and bias errors, a huge number of particles, n_p, was used, i.e., 1 million. Equation (18) is integrated as

$$\boldsymbol{\phi}^{(i)}(t+\Delta t) = [\boldsymbol{\phi}^{(i)}(t) - \boldsymbol{\phi}_c^{(i)}] e^{-\Delta t/\tau_\phi^{(i)}} + \boldsymbol{\phi}_c^{(i)} \tag{22}$$

using $\Delta t = 0.005/\langle\omega\rangle$. Note that the source term $\mathbf{S}(\boldsymbol{\phi}^{(i)})$ is not needed here.

B. Initial conditions

More involved is the generation of initial conditions for the PSP model simulations, which have to be in good agree-

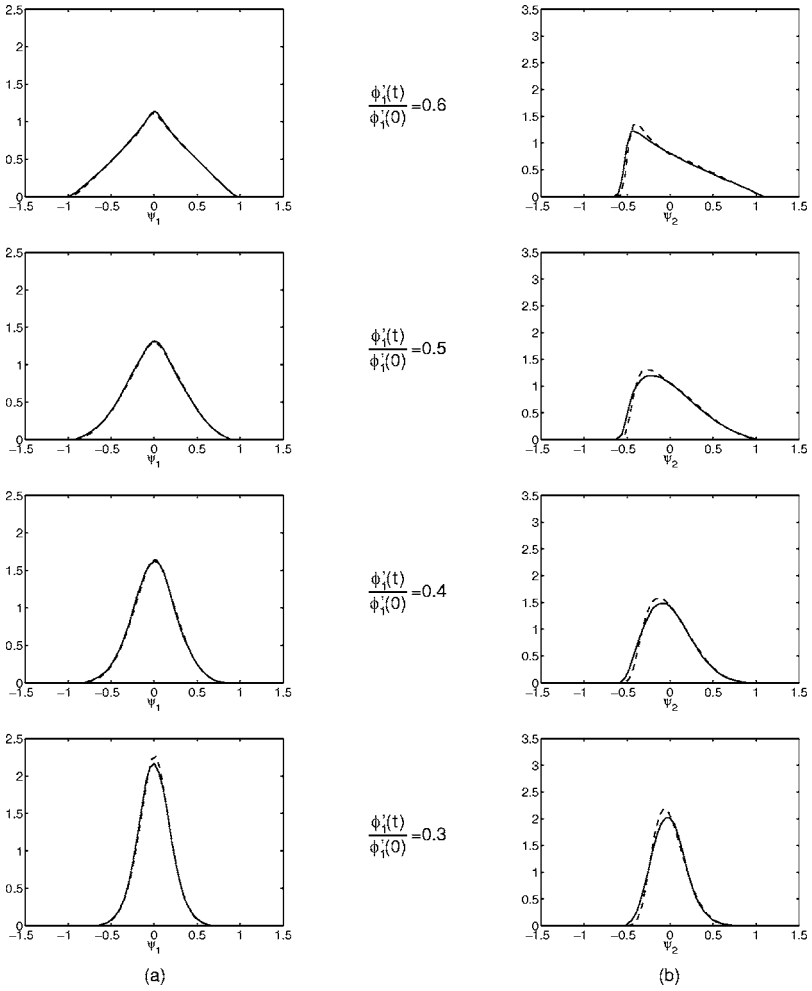

FIG. 9. Marginal PDFs, phase 2; same as Fig. 8.

ment with those of the DNS. Therefore, the procedure described by Eswaran and Pope[9] for one scalar and extended by Juneja and Pope[8] for two scalars was reimplemented. It was used to generate the initial scalar distributions on a three-dimensional spatial grid with $128\times128\times128=2097152$ nodes. The scalar values and their spatial derivatives at all grid nodes provide a large ensemble of samples representing the initial scalar PDF and the according conditional scalar diffusion rate distribution of the DNS. The initial scalar values of all particles in our simulation were obtained by randomly selecting n_p samples. Moreover, the corresponding profile center values were chosen such that the relation

$$(\Gamma\nabla^2\boldsymbol{\phi})^{(i)} = -\frac{1}{\tau_\phi^{(i)}}(\boldsymbol{\phi}^{(i)} - \boldsymbol{\phi}_c^{(i)}) \tag{23}$$

is approximately fulfilled. Here, $(\Gamma\nabla^2\boldsymbol{\phi})^{(i)}$ is the scalar diffusion rate vector of the sample belonging to particle i. More precisely, for every particle a fixed number n_i, of different pairs of profile boundary vectors are randomly selected as described in Sec. III B 1 and Appendix A for a degenerated profile. The pair resulting in the profile center vector closest to the one given by Eq. (23) is chosen. Prandtl number, viscosity and thermal diffusivity were the same as for R48A, i.e., $\mathrm{Pr}=0.7$, $\nu=0.025$ and $\Gamma=\nu/\mathrm{Pr}=0.0357$, respectively. With these steps and $n_i=200$, approximately the same initial

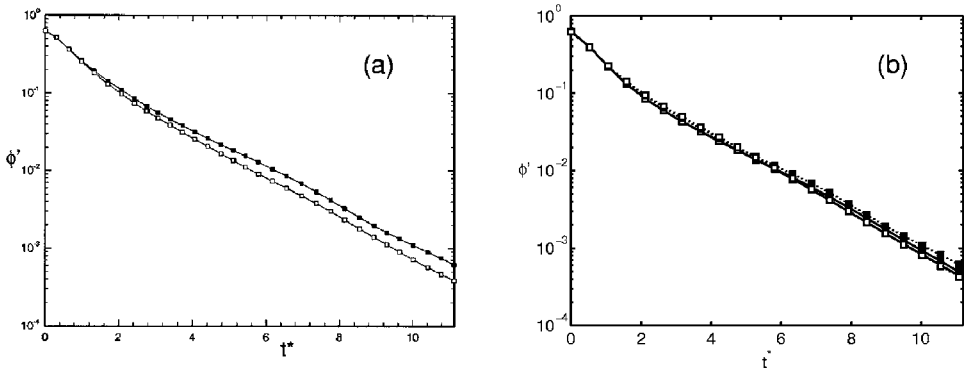

FIG. 10. Scalar rms; (a) DNS R48A by Juneja and Pope (Ref. 8), (b) PSP mixing model; scalar 1 (filled symbols), scalar 2 (hollow symbols); in (b): two-scalar simulation (solid lines), one-scalar simulations (dashed lines).

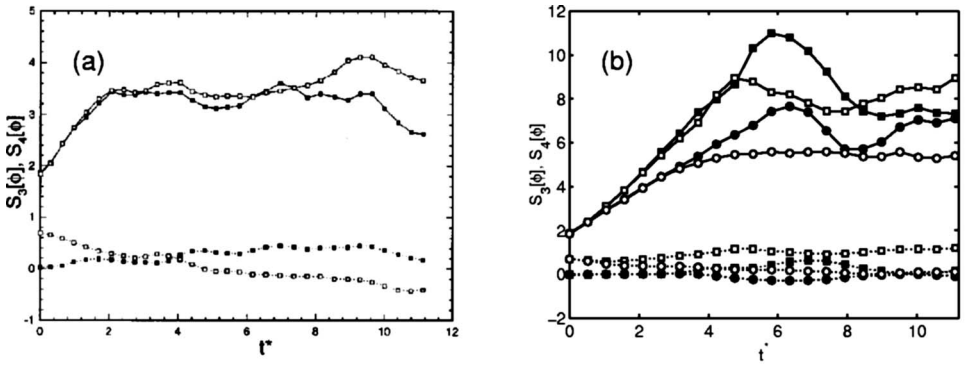

FIG. 11. Normalized skewness (dashed lines) and flatness (solid lines); (a) DNS R48A by Juneja and Pope (Ref. 8), (b) PSP mixing model; scalar 1 (filled symbols), scalar 2 (hollow symbols); in (b): two-scalar simulation (squares), one-scalar simulations (circles).

joint PDF of scalars and conditional scalar diffusion rates as in the DNS are obtained. The time stamps, t_+ and t_-, are initialized as $t_\pm = \zeta/(C_t\omega^{(k)})$, where k is the index of the particle that represents the corresponding profile boundary vector and $\zeta \in [0,1]$ is a uniformly distributed random number.

C. Results

The joint scalar PDF, $f_{\phi_1,\phi_2}(\psi_1,\psi_2;t)$, and the conditional scalar diffusion rate vector, $\boldsymbol{\gamma}(\boldsymbol{\psi};t) = \langle \Gamma\nabla^2\boldsymbol{\phi} \,|\, \boldsymbol{\phi}(t) = \boldsymbol{\psi}\rangle$, were estimated by dividing the ψ_1-ψ_2 sample space into 60×60 bins and sampling particles. In the plots where temporal evolutions are shown the time was normalized by the eddy-turnover time,

$$T = \frac{L_{11}}{L}\frac{L}{u}. \tag{24}$$

The estimation of the Reynolds number dependent ratio of longitudinal and integral length scale, i.e., L_{11}/L, is given in Appendix B for $\mathrm{Re}_\lambda = 48.6$. Moreover, the definitions $L = k^{3/2}/\varepsilon$, $u = \sqrt{2k}$, and $\langle\omega\rangle = \varepsilon/k$ were used.

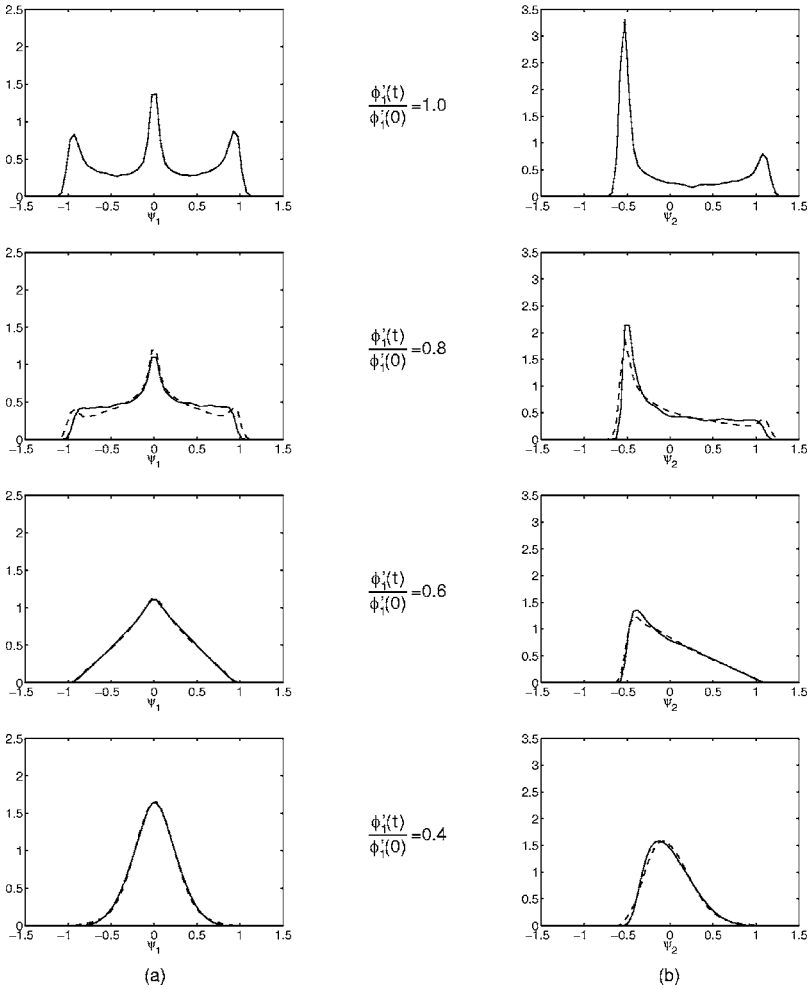

FIG. 12. Marginal PDFs; (a) $f_{\phi_1}(\psi_1;t)$, (b) $f_{\phi_2}(\psi_2;t)$; two-scalar PSP simulation (solid lines), one-scalar PSP simulations (dashed lines).

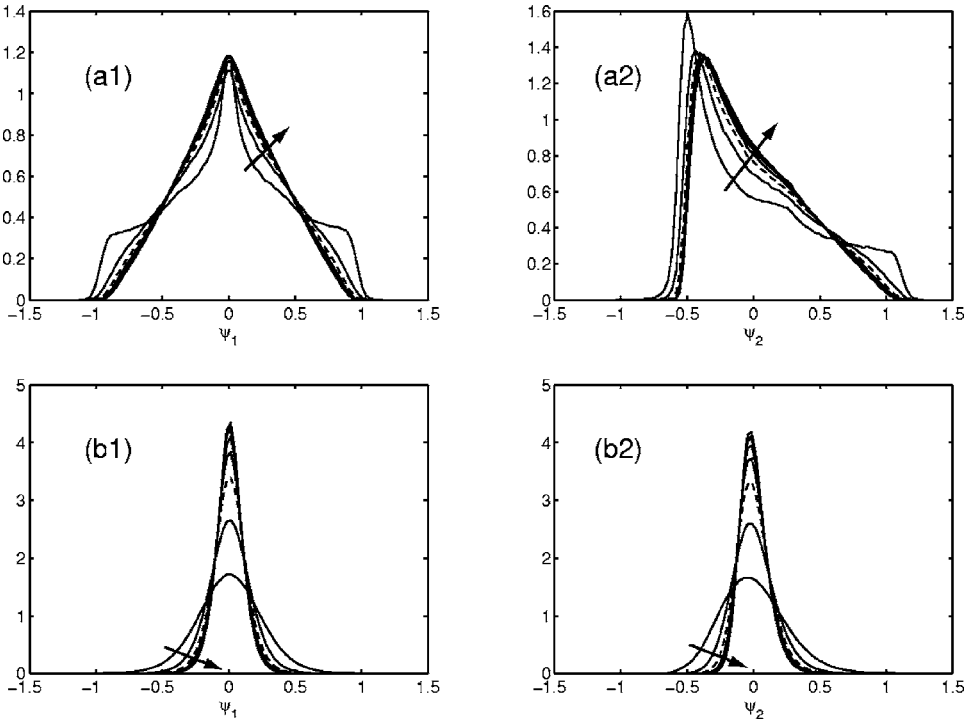

FIG. 13. Averaged marginal PDFs at nondimensional times t^*; (a1, b1) $\widetilde{f}_{\phi_1}(\psi_1;t)$, (a2, b2) $\widetilde{f}_{\phi_2}(\psi_2;t)$; (a1, a2) $t^*=0.7$, (b1, b2) $t^*=2$; arrows indicate direction of increasing $n_p=2^4,2^6,2^8,\ldots,2^{18}$, $n_p=2^8=256$ (dashed lines).

1. Evolution of the joint scalar PDF

In Figs. 4–7 the joint scalar PDF, $f_{\phi_1,\phi_2}(\psi_1,\psi_2;t)$, and the conditional scalar diffusion rate vector, $\boldsymbol{\gamma}(\psi_1,\psi_2;t)$, are compared with the DNS data R92A of Juneja and Pope.[8] The corresponding comparison of the marginal PDFs, $f_{\phi_1}(\psi_1;t)$ and $f_{\phi_2}(\psi_2;t)$, are shown in Figs. 8 and 9. The excellent agreement between PSP results and DNS data supports the physical assumptions in the PSP model. The evolution of the rms values, ϕ_1' and ϕ_2', is depicted in Fig. 10 and compared with the DNS data R48A. The same comparison for the normalized skewness and flatness are shown in Fig. 11. While there is good agreement for second and third moments, deviations can be observed for the fourth moment.

2. Linearity and independence

Although the independence and linearity criterion (v) is not fulfilled by the condition (19), it was investigated if this criterion is at least approximately satisfied at the numerical level. The formulation of the PSP mixing model for multiple scalars described in Sec. III B 3 was applied for one-scalar simulations. To obtain the initial condition the same procedure as discussed in Sec. IV B was employed. The initial PDFs are equivalent to the marginal PDFs of $f_{\phi_1,\phi_2}(\psi_1,\psi_2;t=0)$. From the good agreement between the one- and two-scalar simulations in Figs. 10(b), 11(b), and 12, one can conclude that for this case the independence and linearity requirements are fulfilled satisfactory by the PSP model.

3. Bias error

The sensitivity of the PSP mixing model to bias error was studied using different numbers of particles, i.e., $n_p=2^4,2^5,2^6\ldots2^{21}$. To reduce the statistical error for low n_p, $n_s=2^{21}/n_p$ independent simulations were performed and the results averaged. Like the statistical error, the bias error becomes prominent for small n_p. However, it cannot be reduced by averaging multiple individual simulations. Figure 13 depicts how the averaged marginal PDFs, $\widetilde{f}_{\phi_1}(\psi_1;t)$ and $\widetilde{f}_{\phi_2}(\psi_2;t)$, converge as $n_p\to\infty$ at different times. Especially

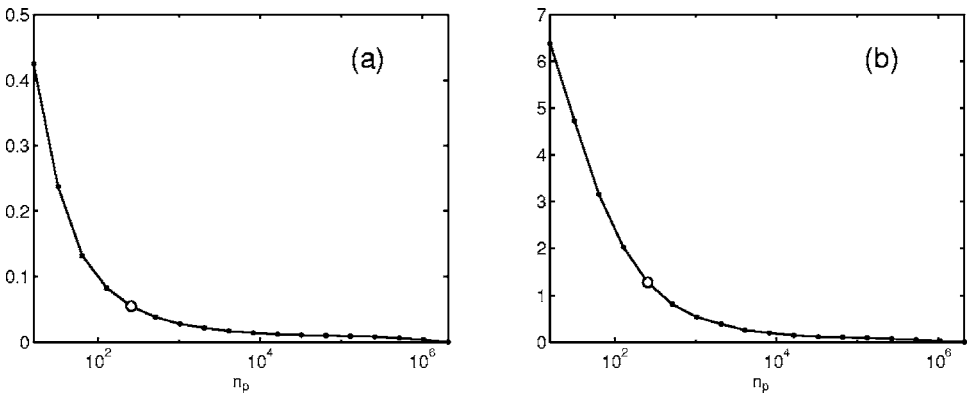

FIG. 14. Bias error estimate, E, as a function of the number of particles, n_p, at nondimensional times t^*; (a) $t^*=0.7$, (b) $t^*=2$; $n_p=2^8=256$ (hollow circles).

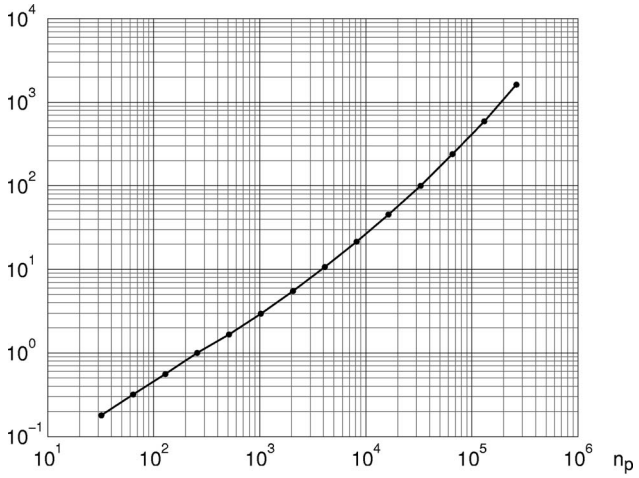

FIG. 15. Normalized CPU time as a function of n_p.

at later times it can be observed that the bias error due to small particle numbers results in a PDF with too large second moments. In fact, the PDF does not collapse in a single peak at a very late time as it should. Note, however, that this is not a particular problem of the PSP model, but results from the fact that the finite particle ensembles used for the individual simulations have different scalar means. Therefore, since the PSP model conserves the mean in each single simulation, at very late times the sampled scalar PDF represents the distribution of these means. For this study, no attempt was made to overcome this inaccuracy, but for large simulations of complex, inhomogeneous cases it would be preferable to apply a correction, e.g., by employing time averaged information.[2] To analyze the bias error quantitatively, we consider the quantity

$$E(n_p) = \int \int_{-\infty}^{\infty} [\tilde{f}^{n_p}_{\phi_1,\phi_2}(\psi_1,\psi_2;t) - \tilde{f}^{r}_{\phi_1,\phi_2}(\psi_1,\psi_2;t)]^2 d\psi_1 d\psi_2. \quad (25)$$

Figure 14 shows a numerical approximation of the bias error estimate, E, as a function of n_p. Note that the PDF $\tilde{f}^{n_p}_{\phi_1,\phi_2}$ is obtained from simulations with n_p particles, while $\tilde{f}^{r}_{\phi_1,\phi_2}$ is the reference (with $n_p=2^{21}$). It can be seen from Figs. 13 and 14 that the bias error becomes reasonably small for particle numbers larger than 256. A similar study was performed to assess the computational efficiency of the PSP mixing model. Figure 15 shows the normalized CPU time as a function of n_p, and it can be observed that it scales linearly up to approximately 10^4 particles.

4. Influence of initial conditional scalar diffusion rates

Here, we study the influence of the initial conditional diffusion rate on the evolution of the joint scalar PDF. Therefore, the test case of Sec. IV C 1 was computed, but this time the same procedure as for the reassignment of degenerated profile boundaries (Sec. III B 1 and Appendix A) was employed for initialization. Figure 16 shows the evolution of the joint scalar PDF as well as the development of the conditional scalar diffusion rate. While one can observe a strong initial deviation from the results of the previous test case (Figs. 6 and 7), the conditional scalar diffusion rates develop consistently and are in reasonable agreement at a later stage. This study shows clearly that for the PSP model not only the initial joint scalar statistics, but also the correct initial conditional diffusion rates have to be honored, which is in agreement with physical observations. In general, however, the joint scalar distribution at the inflow boundaries of PDF simulations is less complex than the initial condition in the homogeneous isotropic mixing test case under consideration, and can be specified.

V. CONCLUSION

The new mixing model presented in this paper achieves closure of molecular diffusion in PDF methods by constructing a statistical picture of one-dimensional scalar profiles. These profiles are assumed to be self-similar and are characterized by a number of parameters, i.e., a length scale and their extreme values, whose dynamics is modeled. The excellent performance of the model was demonstrated by comparing results of a challenging two-scalar mixing test case with corresponding DNS data. In addition to an almost perfect agreement of the joint scalar PDFs, an equally good match was found for the conditional diffusion rates. In the high Reynolds number limit the rms decay rate is predicted correctly if $C'_\phi=15$ is used. In terms of efficiency, it is a great advantage that this mixing model scales almost linearly with the number of particles. Convergence studies indicate that at least 256 particles should be used (for similar test cases) in order to reduce the deterministic bias error to an acceptable level. Moreover, the new mixing model has a number of advantageous properties: the mean of the scalars is preserved [requirement (i)], the scalar variances decay [requirement (ii)], boundedness is satisfied in the one-scalar formulation and only weakly violated in the multiscalar case [requirement (iv)], invariance with respect to rotation in scalar space, and simplicity. In addition, in the one-scalar formulation of the PSP mixing model the picture of sinusoidal scalar profiles is fully applicable (Fig. 2) and therefore conditional quantities depending on spatial gradients like the conditional dissipation rate are available. This is of particular interest when PDF methods are used in combination with flamelet models. Numerical studies revealed that linearity and independence of other inert scalars are fulfilled approximately [requirement (v)], but the fourth statistical moments at late times are not correctly predicted [requirement (iii)]. The PSP mixing model is not local in scalar space [requirement (vi)].

Issues which will be addressed in the near future include dependence on length scale distributions [requirement (vii)], Reynolds and Schmidt numbers [requirement (viii)]. This can be achieved, e.g., by replacing the constant C'_ϕ by an appropriate model. A further topic is the treatment of reactive scalars. The goal will be to deal with reactions in the mixing model directly which would result in a much more rigorous coupling between mixing and reactions. In that case,

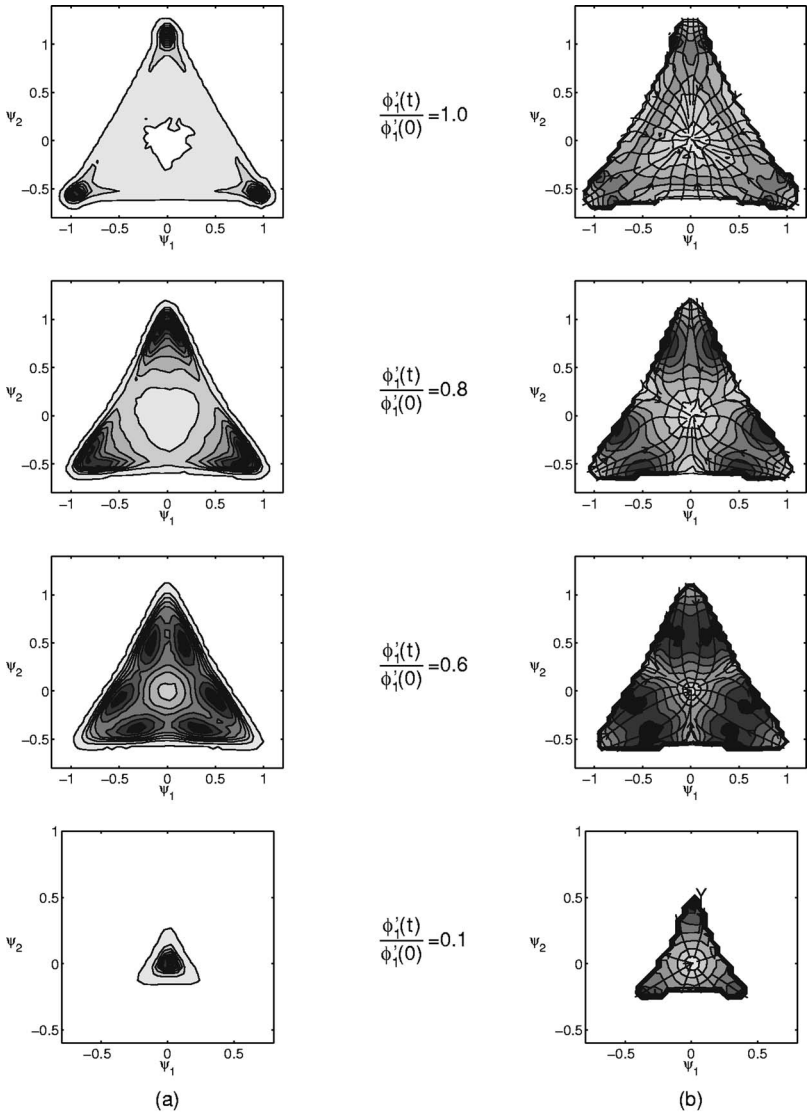

FIG. 16. PSP mixing model without DNS initial condition for $\boldsymbol{\gamma}$; (a) joint PDF $f_{\phi_1,\phi_2}(\psi_1,\psi_2;t)$, (b) conditional scalar diffusion rate $\boldsymbol{\gamma}(\psi_1,\psi_2;t)$; contour levels in (a) and (b), and lines in (b) same as Figs. 4 and 6.

however, the picture of self-similar profiles may no longer be accurate enough and the concept has to be generalized.

ACKNOWLEDGMENTS

This work was supported by the Swiss National Science Foundation. We would particularly like to acknowledge several helpful discussions with Professor R. Fox (Department of Chemical Engineering, Iowa State University) and Professor S. B. Pope (Sibley School of Mechanical and Aerospace Engineering, Cornell University).

APPENDIX A: PROFILE BOUNDARY RENEWAL ALGORITHM

In this appendix an efficient implementation for the profile boundary renewal processes described in Sec. III B 1 is outlined. By replacing condition (12) by (19), the following explanations can be generalized from one to multiple scalars. We consider ensembles of particles that belong to the same computational cell.

If a time stamp, $t_-^{(i)}$ or $t_+^{(i)}$, becomes zero or negative the corresponding profile boundary of particle i, $\phi_-^{(i)}$ or $\phi_+^{(i)}$ has to be replaced. Therefore, we suggest two different approaches:

(A1) To find a new particle for the boundary $\phi_+^{(i)}$, particles are randomly selected from the ensemble (including particle i) until condition (12) is satisfied.

(A2) First, a subensemble with all valid representatives for $\phi_+^{(i)}$ [satisfying condition (12)] is set up. Particle i is included in this subensemble. From the subensemble a new representative for $\phi_+^{(i)}$ is then randomly selected.

If particle i is close to a boundary of the convex hull of the particle distribution in scalar space and $\phi_-^{(i)}$ is near the center, only few valid representatives for $\phi_+^{(i)}$ may be available. Therefore, it is likely that approach A2 is more effective than A1 (vice versa for a particle near the center). Therefore, we use a dual strategy and apply A2 after approach A1 failed in n_{A1} trials with $n_{\mathrm{A1}}=100$. Note that the choice of n_{A1} is only a performance issue and has no influence on the results.

When the scalar profile associated with particle i becomes degenerated, first a new representative particle for $\phi_-^{(i)}$

is randomly selected from the ensemble. Second, the algorithm outlined at the end of the previous paragraph is applied to find $\phi_+^{(i)}$. Note that the profile properties with superscripts + and − are interchangeable.

APPENDIX B: INTEGRAL LENGTH SCALE RATIO

In this Appendix the ratio L_{11}/L is estimated as a function of the Taylor-scale Reynolds number, Re_λ, in order to determine the eddy turnover time, T, which is employed to normalize the time used to present the simulation results. For isotropic turbulence the longitudinal integral length scale, L_{11}, is defined as

$$L_{11} = \frac{3\pi}{4k}\int_0^\infty \frac{E(\kappa)}{\kappa} d\kappa, \tag{B1}$$

where κ is the wave number. For the following analysis the model spectrum

$$E(\kappa) = C\varepsilon^{2/3}\kappa^{-5/3} f_L(\kappa L) f_\eta(\kappa\eta) \tag{B2}$$

is used with the nondimensional functions[1,5]

$$f_L(\kappa L) = \left(\frac{\kappa L}{[(\kappa L)^2 + c_L]^{1/2}}\right)^{5/3+p_0}$$
$$\text{and} \quad f_\eta(\kappa\eta) = \exp(-\beta\{[(\kappa\eta)^4 + c_\eta^4]^{1/4} - c_\eta\}), \tag{B3}$$

the dissipation rate ε, the Kolmogorov length scale η, and the model parameters C, c_L, c_η, p_0, and β. While c_L and c_η are Reynolds number dependent, C, p_0, and β are constants that are typically taken to be 1.5, 2, and 5.2, respectively. The relations between the turbulent kinetic energy, k, the dissipation rate, ε, and the energy spectrum, $E(\kappa)$, are given by

$$k = \int_0^\infty E(\kappa) d\kappa \quad \text{and} \quad \varepsilon = \int_0^\infty 2\nu\kappa^2 E(\kappa) d\kappa, \tag{B4}$$

where ν is the kinematic viscosity. Using the definition of the Taylor-scale Reynolds number, Re_λ, one can express the length scale ratio

$$\frac{L}{\eta} = \left(\frac{20}{3}\right)^{-3/4} \mathrm{Re}_\lambda^{3/2}. \tag{B5}$$

Finally, by introducing the variable $\xi = \kappa\eta$, one can reexpress (B4) using (B2) and (B3) as

$$\frac{\mathrm{Re}_\lambda}{C}\left(\frac{3}{20}\right)^{1/2} = \int_0^\infty \xi^{-5/3} f_L(\xi L/\eta) f_\eta(\xi) d\xi$$
$$\text{and} \quad \frac{1}{2C} = \int_0^\infty \xi^{1/3} f_L(\xi L/\eta) f_\eta(\xi) d\xi. \tag{B6}$$

This is a nonlinear system that allows to determine c_L and c_η. Similarly, by using definition (B1), the ratio L_{11}/L can be expressed by

$$\frac{L_{11}}{L} = \frac{3\pi C}{4}\left(\frac{20}{3}\right)^{5/4} \mathrm{Re}_\lambda^{-5/2} \int_0^\infty \xi^{-8/3} f_L(\xi L/\eta) f_\eta(\xi) d\xi. \tag{B7}$$

As a result from this analysis, one obtains for $\mathrm{Re}_\lambda = 48.6$ the values of c_L, c_η, and L_{11}/L, which are 3.948, 0.4304, and 0.6694, respectively.

[1] S. B. Pope, *Turbulent Flows* (Cambridge University Press, Cambridge, 2000).
[2] P. Jenny, S. B. Pope, M. Muradoglu, and D. A. Caughey, "A hybrid algorithm for the joint PDF equation of turbulent reactive flows," J. Comput. Phys. **166**, 218 (2001).
[3] P. Jenny, M. Muradoglu, K. Liu, S. B. Pope, and D. A. Caughey, "PDF simulations of a bluff-body stabilized flow," J. Comput. Phys. **169**, 1 (2001).
[4] S. B. Pope, "Lagrangian PDF methods for turbulent flows," Annu. Rev. Fluid Mech. **26**, 23 (1994).
[5] R. O. Fox, *Computational Models for Turbulent Reacting Flows* (Cambridge University Press, Cambridge, 2003).
[6] S. Subramaniam and S. B. Pope, "A mixing model for turbulent reactive flows based on Euclidean minimum spanning trees," Combust. Flame **115**, 487 (1998).
[7] A. T. Norris and S. B. Pope, "Turbulent mixing model based on ordered pairing," Combust. Flame **83**, 27 (1991).
[8] A. Juneja and S. B. Pope, "A DNS study of turbulent mixing of two passive scalars," Phys. Fluids **8**, 2161 (1996).
[9] V. Eswaran and S. B. Pope, "Direct numerical simulations of the turbulent mixing of a passive scalar," Phys. Fluids **31**, 506 (1988).
[10] P. K. Yeung, "Lagrangian characteristics of turbulence and scalar transport in direct numerical simulations," J. Fluid Mech. **427**, 241 (2001).
[11] R. L. Curl, "Dispersed phase mixing: 1. Theory and effects in simple reactors," AIChE J. **9**, 175 (1963).
[12] J. Villermaux and J. C. Devillon, "Representation de la coalescence et de la redispersion des domaines de segregation dans un fluide par un modele d'interaction phenomenologique," in *Second International Symposium on Chemical Reaction Engineering* (Elsevier, New York, 1972), p. 1.
[13] C. Dopazo and E. E. O'Brien, "Approach to autoignition of a turbulent mixture," Acta Astronaut. **1**, 1239 (1974).
[14] S. B. Pope, "Mapping closures for turbulent mixing and reaction," Theor. Comput. Fluid Dyn. **2**, 255 (1991).
[15] J. Xu and S. B. Pope, "PDF calculations of turbulent nonpremixed flames with local extinction," Combust. Flame **123**, 281 (2000).
[16] Z. Y. Ren and S. B. Pope, "An investigation of the performance of turbulent mixing models," Combust. Flame **136**, 208 (2004).
[17] S. Mitarai, J. J. Riley, and G. Kosaly, "Testing of mixing models for Monte Carlo probability density function simulations," Phys. Fluids **17**, 47101 (2005).
[18] K. Liu, S. B. Pope, and D. A. Caughey, "Calculations of bluff-body stabilized flames using a joint probability density function model with detailed chemistry," Combust. Flame **141**, 89 (2005).
[19] A. Y. Klimenko and S. B. Pope, "The modeling of turbulent reactive flows based on multiple mapping conditioning," Phys. Fluids **15**, 1907 (2003).
[20] R. O. Fox, "The Fokker-Planck closure for turbulent molecular mixing—passive scalars," Phys. Fluids A **4**, 1230 (1992).
[21] R. O. Fox, "Improved Fokker-Planck model for the joint scalar, scalar gradient PDF," Phys. Fluids **6**, 334 (1994).
[22] R. O. Fox and P. K. Yeung, "Improved Lagrangian mixing models for passive scalars in isotropic turbulence," Phys. Fluids **15**, 961 (2003).
[23] S. Heinz, "On Fokker-Planck equations for turbulent reacting flows. Part 1. Probability density function for Reynolds-averaged Navier-Stokes equations," Flow, Turbul. Combust. **70**, 115 (2003).
[24] S. Heinz, *Statistical Mechanics of Turbulent Flows* (Springer, Berlin, 2003).
[25] S. B. Pope, "Advances in PDF methods for turbulent reactive flows," in *Tenth European Turbulence Conference*, edited by H. Andersson and P.-A Krogstad (CIMNE, Trondheim, 2004), p. 529.
[26] D. W. Meyer and P. Jenny, "Stochastic mixing model for PDF simulations of turbulent reactive flow," in *Tenth European Turbulence Conference*, edited by H. Andersson and P.-A. Krogstad (CIMNE, Trondheim, 2004), p. 681.
[27] Jayesh and S. B. Pope, "Stochastic model for turbulent frequency," Tech-

nical Report No. FDA 95-05, Cornell University (1995).
[28]R. O. Fox, "The Lagrangian spectral relaxation model of the scalar dissipation in homogeneous turbulence," Phys. Fluids **9**, 2364 (1997).
[29]R. O. Fox, "Computation of turbulent reactive flows: first-principles macro/micromixing models using probability density function methods," Chem. Eng. Sci. **47**, 2853 (1992).
[30]K. Nipp and D. Stoffer, *Lineare Algebra*, 4th ed. (VDF Hochschulverlag an der ETH, Zurich, 1998).